

## ARTICLE



# Inhibition of TXNDC5 attenuates lipopolysaccharide-induced septic shock by altering inflammatory responses

Yanping Zeng<sup>1</sup>✉, Weixing Ma<sup>1</sup>, Cheng ma<sup>1</sup>, Xiaohui Ren<sup>1</sup> and Yan Wang<sup>1</sup>

© The Author(s), under exclusive licence to United States and Canadian Academy of Pathology 2021

Sepsis and its severe form, septic shock, represent the leading cause of death among hospitalized patients. Thioredoxin is a ubiquitous protein essential for cellular redox balance and its aberrant expression is associated with a wide spectrum of inflammation-related pathological conditions. The current study aimed to compare the expression of thioredoxin domain containing 5 (TXNDC5) in septic patients with or without septic shock and to explore the potential regulatory effects of TXNDC5 in sepsis. We analyzed the RNA expression data downloaded from the Gene Expression Omnibus database and measured the plasma level of TXNDC5 in septic patients. The results showed that TXNDC5 was upregulated in patients with septic shock compared to septic patients without shock or healthy controls. We further treated wild-type mice and cultured macrophages with lipopolysaccharide (LPS) and found that TXNDC5 was highly expressed in mice with LPS-induced sepsis and macrophages subjected to LPS stimulation compared to corresponding controls. Then a mouse strain with targeted depletion of *Txndc5* was generated. *Txndc5* depletion reduced inflammatory cytokine production and affected the recruitment of macrophages and neutrophils into the blood and peritoneum of mice challenged with LPS. Further analysis revealed that TXNDC5 inhibition alleviated LPS-induced sepsis by inhibiting the NF- $\kappa$ B signaling pathway. In summary, these findings suggested that the inhibition of TXNDC5 may be a potential approach to treat sepsis and related syndromes.

*Laboratory Investigation* (2022) 102:422–431; <https://doi.org/10.1038/s41374-021-00711-5>

## INTRODUCTION

Sepsis is a life-threatening syndrome caused by dysregulated host immune responses to infection<sup>1,2</sup>. This complex and highly coordinated process involves a multitude of events, including immune response, bacterial or endotoxin clearance, and tissue remodeling<sup>3</sup>. The increase in endotoxin levels during sepsis drives the activation of innate immune cells, resulting in the production of inflammatory cytokines associated with multiple organ failure and a high risk of death<sup>4</sup>. Septic shock is the most severe form of sepsis characterized by decreased systemic vascular resistance, vascular leakage, myocardial dysfunction, and severe hypotension<sup>5</sup>. It represents the leading cause of death among critically ill patients hospitalized in the intensive care unit, with the mortality approaching 50%<sup>6</sup>. Thus, a more comprehensive understanding of the pathological process of sepsis may contribute to the rapid diagnosis and development of new therapeutic strategies for this disease.

Macrophages play an essential role throughout all stages of sepsis, involving both inflammatory responses and immune homeostasis<sup>7</sup>. They are activated in response to a variety of stimuli, such as Gram-negative bacteria and lipopolysaccharide (LPS), resulting in the upregulation of inflammatory genes<sup>8</sup>. At the early stage of sepsis, macrophages undergo M1 differentiation, promoting host immune defense by releasing large amounts of proinflammatory cytokines, such as interleukin (IL)-6, monocyte chemoattractant protein-1 (MCP-1), and tumor necrosis factor alpha (TNF- $\alpha$ )<sup>9</sup>. However, excessive activation of proinflammatory macrophages may lead to a “cytokine storm,” during which both

affected and healthy tissues are attacked<sup>10</sup>. Concordantly, activated proinflammatory macrophages polarize to the M2 phenotype, which induces the production of anti-inflammatory cytokines (e.g., IL-10) and promote the process of immunosuppression to minimize host tissue damage<sup>11</sup>. Therefore, prevention of excess immune cell activation can be of great benefit for sepsis-induced immunopathology.

Thioredoxin is a class of small ubiquitous proteins that plays a critical role in regulating cellular redox balance<sup>12</sup>. Thioredoxin domain containing 5 (TXNDC5) is an endoplasmic reticulum-resident protein that belongs to the thioredoxin family, responsible for the proper folding of many proteins with disulfide bonds<sup>13</sup>. The aberrant expression of TXNDC5 is associated with a wide range of pathological conditions, including cancers, arthritis, neurodegenerative diseases, and infection<sup>14</sup>. Previous evidence suggests that TXNDC5 is a proinflammatory factor that promotes abnormal cell differentiation, angiogenesis, and bone destruction in rheumatoid arthritis (RA) synovium<sup>15</sup>. Moreover, it has been reported that TXNDC5 exacerbates the inflammatory phenotype of synovial fibroblasts in RA via regulating the activity of the NF- $\kappa$ B pathway<sup>16</sup>. However, whether TXNDC5 is involved in sepsis-induced inflammation and organ damage has not been reported yet.

In this study, we identified *Txndc5* as a differentially expressed gene (DEG) in septic shock by analyzing the RNA expression data downloaded from the Gene Expression Omnibus (GEO) database and comparing the expression of TXNDC5 in septic patients with

<sup>1</sup>Department of ICU, Shaoxing Central Hospital Medical Alliance General Hospital, Shaoxing, Zhejiang 312030, China. ✉email: zengyanping0621@163.com

Received: 23 June 2021 Revised: 16 November 2021 Accepted: 22 November 2021

Published online: 4 December 2021

or without septic shock. Then we explored the effect of *TxnDC5* depletion on LPS-induced sepsis in mice and cultured macrophages. The modulation of TXNDC5 in the NF- $\kappa$ B signaling was also investigated. Our findings highlighted an alternative approach to treat sepsis by inhibiting the expression of TXNDC5.

## MATERIALS AND METHODS

### Ethical statement

All procedures involving human participants were approved by the Ethics Committee of the Shaoxing Central Hospital Medical Alliance General Hospital, and performed in accordance with the Declaration of Helsinki<sup>17</sup>. All subjects provided written informed consent prior to enrollment. All experiments involving the use of animals were approved by the Animal Care and Use Committee of Shaoxing Central Hospital Medical Alliance General Hospital, and performed following the Guide for the Care and Use of Laboratory Animals<sup>18</sup>.

### Sepsis RNA expression data

The whole-blood RNA expression data were downloaded from the GEO (<http://www.ncbi.nlm.nih.gov/geo/>). The GSE131761 dataset, comprising the expression profiles of septic shock samples ( $n = 81$ ) and non-septic shock samples ( $n = 33$ ), was used to identify DEGs in septic shock using the R package "limma" as previously published<sup>19</sup>. A  $|\log_2(\text{fold change (FC)})| > 1$  and a false-discovery rate (FDR) of  $< 0.05$  indicated statistically significant.

### Clinical samples

Thirty adult patients who were diagnosed with sepsis (15 were septic shock, 15 were non-septic shock) according to the Third International Consensus Definitions for Sepsis and Septic Shock (Sepsis-3)<sup>20</sup> in our hospital were recruited. All procedures involving human participants were approved by the Ethics Committee of the Shaoxing Central Hospital Medical Alliance General Hospital. Peripheral blood samples were obtained from all septic patients at admission. Fifteen age- and gender-matched healthy volunteers

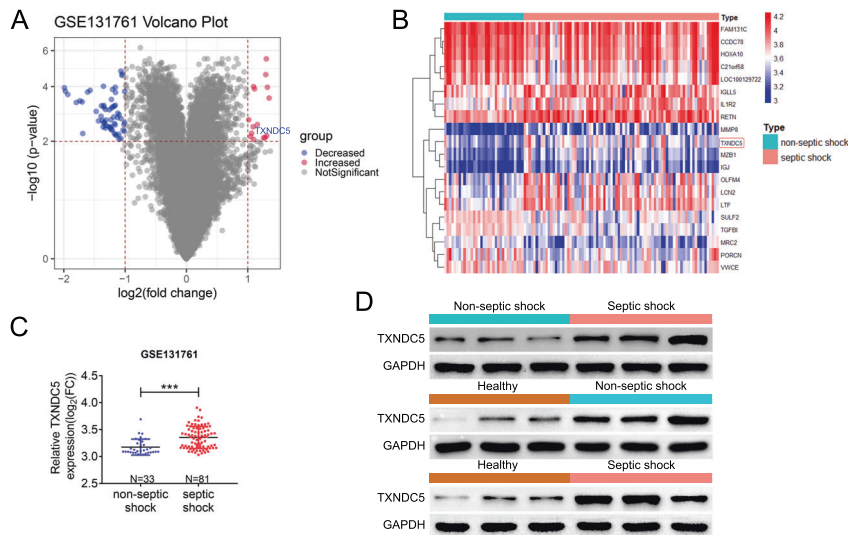


**Fig. 1** Expression of TXNDC5 in patients with sepsis or septic shock, and healthy controls. **A**, **B** The GSE131761 dataset was used to identify DEGs in septic shock. **A** The volcano plot of DEGs in septic shock is generated. Red plots represent aberrantly expressed mRNAs with  $\text{FDR} < 0.05$  and  $\log_2 \text{FC} > 1$ . Blue plots represent aberrantly expressed mRNAs with  $\text{FDR} < 0.05$  and  $\log_2 \text{FC} < -1$ . Black plots represent normally expressed mRNAs. **B** Heatmap analysis showed differential expression profiles in septic shock versus non-septic shock samples. **C** The relative expression of TXNDC5 in the samples from GSE131761 (non-septic shock,  $n = 33$ ; septic shock,  $n = 81$ ) was compared. **D** Peripheral blood samples were collected from 15 patients with sepsis, 15 patients with septic shock, and 15 healthy controls. **E** The protein expression of TXNDC5 in the PBMCs of patients with septic shock or non-septic shock, or healthy controls was assessed by western blot. \*\*\* $p < 0.001$ .

**Table 1.** Demographic and clinical characteristic of patients.

Variables	Non-septic shock (n = 15)	Septic shock (n = 15)	p value
Age, mean (SD)	54.6 (13.38)	59.9 (13.91)	0.996
Gender			
Male	9	7	0.464
Female	6	8	
Lactate (mg/dL), median (IQR)	1.3 (0.3)	1.9 (1.3)	<0.001
PCT (ng/mL), median (IQR)	0.704 (0.135)	16.198 (6.388)	<0.001
CitH3 (pg/mL), median (IQR)	17.4 (7.6)	94.6 (22.6)	0.006
Survivors, n (%)	14 (93.3)	8 (53.3)	0.018
Mechanical ventilation, n (%)	0 (0)	5 (33.3)	0.021
Length of hospital stay (days), median (IQR)	2 (1)	8 (5)	<0.001
Total SOFA, median (IQR)	1 (2)	5 (7)	0.002
SOFA components			
Respiratory, median (IQR)	0 (1)	1 (1)	<0.001
Renal, median (IQR)	0 (1)	2 (1)	0.004
Cardiovascular, median (IQR)	0 (0)	2 (1)	<0.001
Neurologic, median (IQR)	0 (0)	1 (1)	0.002
Hepatic, median (IQR)	0 (0)	0 (1)	0.046
Coagulation, median (IQR)	0 (0)	0 (1)	0.024

were also enrolled from the Medical Examination Center of the same hospital as the control group, and their blood samples were obtained during physical examination. The protein expression of TXNDC5 in peripheral blood mononuclear cells (PBMCs) was measured by western blot.

### Generation of *TxnDC5*<sup>-/-</sup> mice

Wild-type (WT) C57BL/6J mice were purchased from Shanghai Laboratory Animal Center of the Chinese Academy of Sciences and housed in an environment-controlled facility (22 ± 2 °C; 50% ± 10% humidity; 12-h alternating light/dark cycle) with ad libitum access to food and water. A C57BL/6J mouse strain with targeted depletion of *TxnDC5* was generated using clustered regularly interspaced short palindromic repeats (CRISPR)/CRISPR-associated protein 9 (Cas9) genome editing technology as previous described<sup>13</sup>. In brief, purified Cas9 mRNA and two single-guide RNAs targeting introns 1 and 3 of *TxnDC5* were co-injected into one-cell C57BL/6J mouse zygotes using a Piezo impact-driven micromanipulator to generate mice with a large deletion spanning exons 2 and 3 of *TxnDC5*. The injected

blastocysts were then transferred into the uterus of pseudopregnant female mice at 2.5 d.p.c. PCR and DNA sequencing analysis were performed to identify founders harboring an allele with a 6.8 kb deletion encompassing exons 2 and 3 of *TxnDC5*. The founder was crossed to WT C57BL/6J strain to obtain *TxnDC5*<sup>+/-</sup> offspring. Then, the F1 *TxnDC5*<sup>+/-</sup> progeny were crossed to generate homozygous *TxnDC5*<sup>-/-</sup> mice.

### LPS-induced sepsis in mice

Sepsis was induced in male WT C57BL/6J mice (6–8 weeks old, 20–22 g) by a single intraperitoneal injection of LPS (Sigma-Aldrich, St. Louis, USA) at a dose of 10 mg/kg body weight. The mRNA and protein levels of TXNDC5 in the blood, liver, kidney, lung, heart, spleen, pancreas, and stomach were measured at 12-h post injection (*n* = 4 per group). The mRNA levels of TXNDC5 in the blood at different time points (0, 1, 3, 6, 12, and 24 h) following injection were detected by qRT-PCR (*n* = 4 per group per time point).

Six- to eight-week-old male WT mice and aged-matched *TxnDC5*<sup>-/-</sup> mice were administered with 10 mg/kg LPS via intraperitoneal injection. The

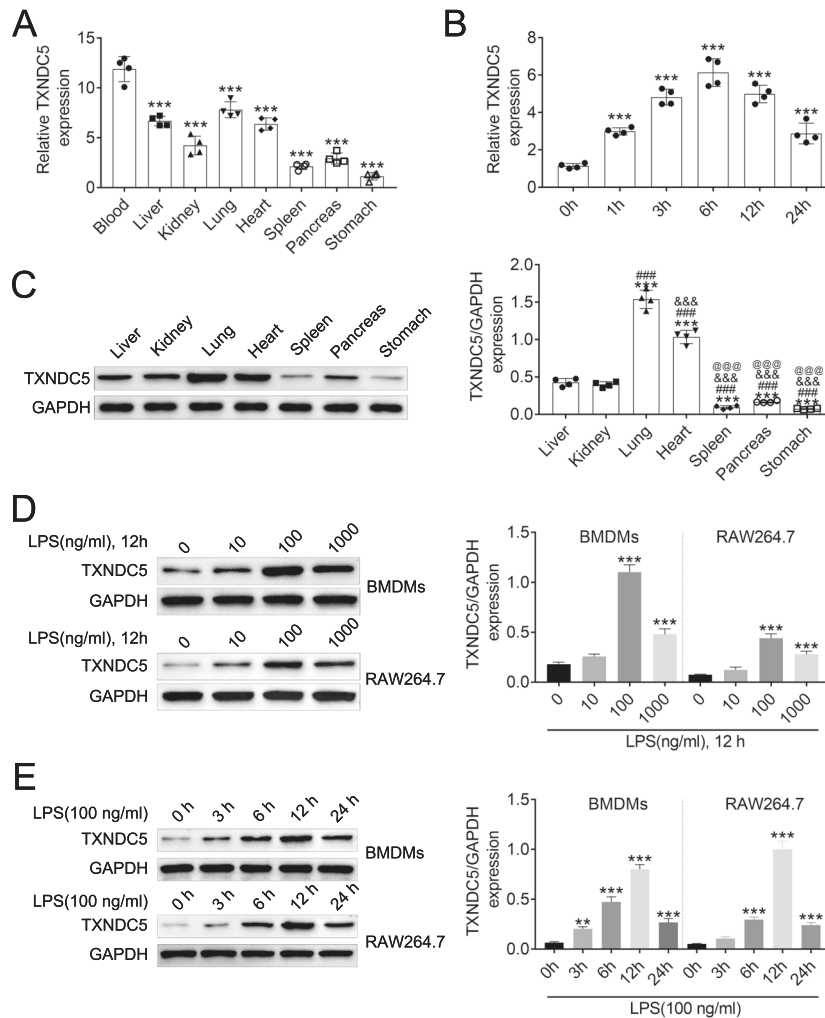


**Fig. 2** Expression of TXNDC5 in LPS-treated mice and macrophages. **A** Male WT mice were administered with LPS (10 mg/kg body weight) via intraperitoneal injection. The mRNA expression of TXNDC5 in the blood, liver, kidney, lung, heart, spleen, pancreas, and stomach was measured at 12-h post injection using qRT-PCR (*n* = 4 per group). \*\*\**p* < 0.001 compared to the “Blood” group. **B** Male WT mice were intraperitoneally injected with LPS (10 mg/kg body weight). The mRNA level of TXNDC5 in the blood was determined by qRT-PCR at 0, 1, 3, 6, 12, and 24 h following treatment (*n* = 4 per group per time point). \*\*\**p* < 0.001 compared to the “0h” group. **C** Male WT mice were injected with LPS (10 mg/kg body weight) via intraperitoneal injection. Western blot analysis was performed to assess the protein expression of TXNDC5 in the liver, kidney, lung, heart, spleen, pancreas, and stomach at 12 h after injection (*n* = 4 per group). \*\*\**p* < 0.001 compared to the “Liver” group. ###*p* < 0.001 compared to the “Kidney” group. &&&*p* < 0.001 compared to the “Lung” group. @@@*p* < 0.001 compared to the “Heart” group. **D** BMDMs isolated from WT mice and RAW264.7 cells were treated with or without LPS at increasing concentrations (10, 100, and 1000 ng/mL) for 12 h. The protein level of TXNDC5 in cells was measured by western blot. \*\*\**p* < 0.001 compared to the “0 ng/mL” group. **E** Mouse BMDMs and RAW264.7 cells were induced with LPS at 100 ng/mL for different periods of time (0, 3, 6, 12, and 24 h). The protein level of TXNDC5 was assessed by western blot. \*\*\**p* < 0.001 compared to the “0h” group.

corresponding control groups were injected with the same volume of phosphate-buffered saline (PBS, Sigma-Aldrich). The survival of all groups was monitored for 1 week and presented as Kaplan–Meier curves. The blood was collected from each animal immediately after death or euthanasia. Peritoneal fluids were harvested as previously published<sup>21</sup>. Briefly, a ventral midline incision was made with scissors and the intact peritoneal wall was exposed. Then 10 mL of harvest solution (0.02% EDTA in 1× PBS) was injected into the abdominal cavity of the target mouse. After gentle massage, peritoneal fluids were withdrawn. The lung, liver, kidney, heart, spleen, pancreas, stomach, and peritoneal tissues were harvested. Tissues subjected to histological examination were fixed in 10% formalin, embedded with paraffin, and stained for hematoxylin and eosin as previously described ( $n = 12$  per group)<sup>22</sup>. Tissue samples subjected to TUNEL staining were sectioned and stained with both TUNEL (Roche, Basel, Switzerland) and DAPI (Thermo Fisher Scientific, Waltham, USA) reagents following the manufacturer's instructions ( $n = 12$  per group). TUNEL-positive cells were counted under a fluorescence microscope: The percentage of TUNEL-positive cells = (number of TUNEL-positive cells)/(number of DAPI-stained nuclei) × 100. The concentrations of TNF- $\alpha$ , IL-10, interferon- $\gamma$  (IFN- $\gamma$ ), IL-12, IL-6, and MCP-1 in the peritoneal tissues and plasma samples were measured by the Quantikine Enzyme-Linked Immunosorbent Assay (ELISA) Kits (R&D Systems, Minneapolis, USA) ( $n = 8$  per group). The expressions of TXNDC5, phospho-I $\kappa$ B $\beta$  (p-I $\kappa$ B $\beta$ ), I $\kappa$ B $\beta$ , phospho-p65 (p-p65), and p65 were determined by western blot.

### Isolation of macrophages and neutrophils

Macrophages and neutrophils were isolated from the blood and peritoneal fluids of mice as previously reported<sup>21</sup>. In brief, peritoneal exudate cells and buffy coat cells were obtained from the pooled peritoneal fluids and the blood samples, respectively, by centrifugation at 200 × g for 10 min. Cells ( $3\text{--}5 \times 10^7$ ) were suspended in 1 mL PBS, and then mixed with 9 mL Percoll gradient solution (GE Healthcare, Chicago, USA) in a 10-mL Beckman ultracentrifuge tube. Macrophages and neutrophils were obtained from different layers after ultracentrifugation.

Flow cytometry was performed to assess the percentages of macrophages (CD11b<sup>+</sup>F4/80<sup>+</sup>) and neutrophils (CD11b<sup>+</sup>Ly6G<sup>+</sup>) in the blood and peritoneal fluids ( $n = 8$  per group) using a FACSArray<sup>TM</sup> bioanalyzer (BD Bioscience, San Jose, USA) as previously reported<sup>23</sup>. The following monoclonal antibodies conjugated to fluorochromes (BioLegend, San Diego, USA) were used: PE-labeled anti-F4/80, PE/Cy7-labeled anti-CD11b, and APC-labeled anti-Ly6G. Data were analyzed using FlowJo (Tree Star, Ashland, USA).

### Cell culture and transfection

Mouse bone marrow-derived macrophages (BMDMs) were obtained by flushing the femur and tibia of WT C57BL/6 mice with DMEM (Invitrogen, Carlsbad, USA) containing 10% fetal bovine serum (FBS, Invitrogen) as previously published<sup>24</sup>. Then isolated cells were filtered through a 70- $\mu$ m cell strainer (Thermo Fisher Scientific, Waltham, USA), washed with PBS,

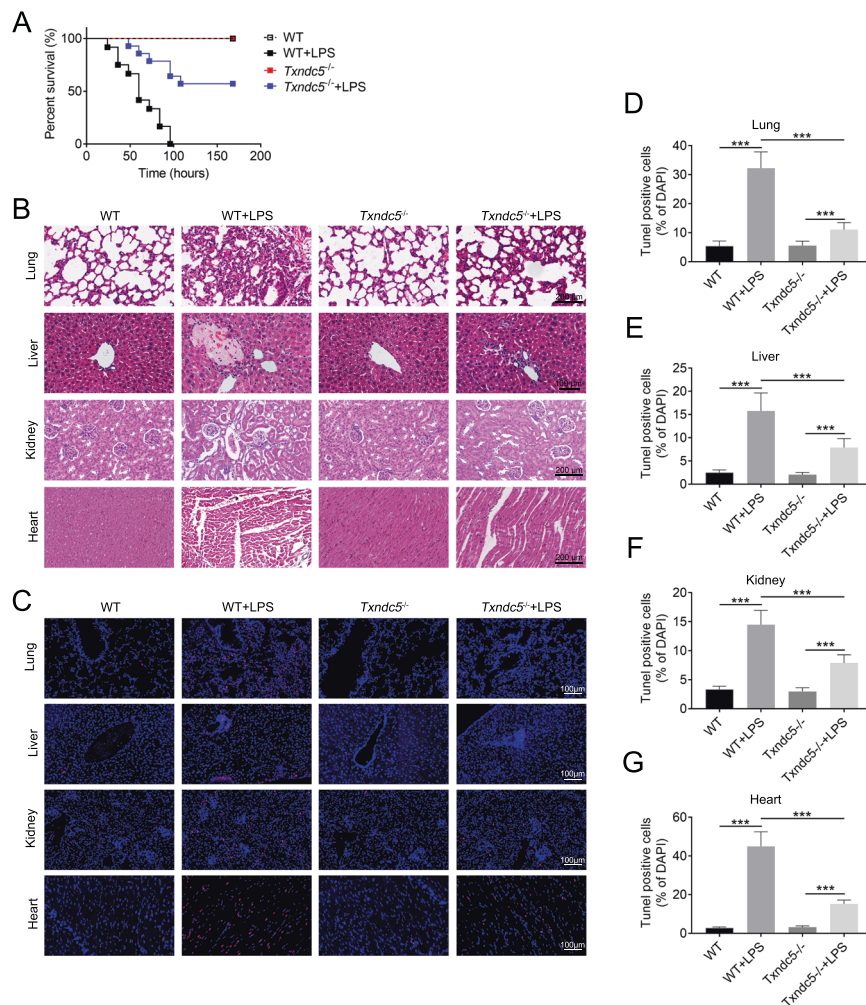


**Fig. 3** Effect of *TxnDC5* depletion on sepsis-induced organ damage in mice. *TxnDC5*<sup>-/-</sup> mice were generated using CRISPR/Cas9 genome editing technology. WT and *TxnDC5*<sup>-/-</sup> mice (6–8 weeks old) were administered with LPS (10 mg/kg body weight) via intraperitoneal injection. The corresponding control groups were injected with the same volume of PBS ( $n = 12$  per group). **A** The survival of all groups was monitored for 7 days and presented as Kaplan–Meier curves. **B** The lung, liver, kidney, and heart were harvested from all animals immediately after death or euthanasia. Samples were assessed for tissue damage by H&E staining. **C** TUNEL staining was performed to assess apoptosis in tissues. TUNEL was a marker of apoptosis (red) and DAPI was used for nuclear counterstain (blue). The percentage of TUNEL-positive cells in the **D** lung, **E** liver, **F** kidney, and **G** heart tissues. \*\*\* $p < 0.001$ .

and maintained in DMEM supplemented with 10% FBS in a 5% CO<sub>2</sub>/37 °C incubator for 1 week to ensure complete differentiation to BMDMs. A density of 2–5 × 10<sup>5</sup> cells/mL was used for subsequent experiments. Mouse macrophage cell line RAW264.7 were purchased from ATCC (Manassas, USA) and cultivated in DMEM containing 10% FBS.

Short hairpin RNA (shRNA) targeting TXNDC5 and scrambled control sequence were synthesized by GenePharma (Shanghai, China) and transfected into BMDMs or RAW264.7 cells using Lipofectamine<sup>®</sup> 2000 Transfection Reagent (Invitrogen). Transfection efficiency was evaluated by qRT-PCR and/or western blot prior to further analyses.

### LPS treatment in vitro

BMDMs and RAW264.7 cells were treated with or without LPS at increasing concentrations (10, 100, and 1000 ng/mL) for 12 h, or induced with LPS at 100 ng/mL for different periods of time (0, 3, 6, 12, and 24 h). The expression of TXNDC5 was determined by western blot.

WT or transfected BMDMs and RAW264.7 cells were treated with LPS (100 ng/mL) for 12 h. The levels of TNF- $\alpha$ , IFN- $\gamma$ , IL-10, IL-12, IL-6, and MCP-1 were assessed by qRT-PCR. The expressions of TXNDC5, p-Ik $\beta$ B, Ik $\beta$ B, p-p65,

and p65 were measured by western blot. Immunofluorescence staining was performed to detect the expression of p65 in all groups of cells following LPS treatment. Cells were fixed with 4% paraformaldehyde, permeabilized with 0.4% Triton X-100 (Sigma-Aldrich), and then stained with anti-p65 antibody (1/100; ab32536, Abcam, Cambridge, USA) and DAPI (nuclei dye, Thermo Fisher Scientific). The signals were detected using a fluorescence microscope (Olympus, Tokyo, Japan).

### qRT-PCR

Total RNA was isolated from tissue samples or whole-cell lysates by Trizol (Invitrogen). The PureLink<sup>™</sup> Total RNA Blood Kit (Thermo Fisher Scientific) was used to extract RNA from blood samples. RNA was reverse transcribed to cDNA using Maxima First Strand cDNA Synthesis Kit (Thermo Fisher Scientific). qRT-PCR was performed using the 7300 Real-Time PCR System (Applied Biosystem, Foster City, USA). The expression of the *Txn5* gene was normalized to the *Gapdh* gene. The following primers were used: *Txn5* forward: 5'-TGAGCCACGGGTGACAAGG-3', *Txn5* reverse: 5'-GC CACACCACGGAGCATAGAAC-3'; *Gapdh* forward: 5'-ATCACTGCCACCCAG AAGAC-3', *Gapdh* reverse: 5'-TTTCTAGACGGCAGGTACAGG-3'.

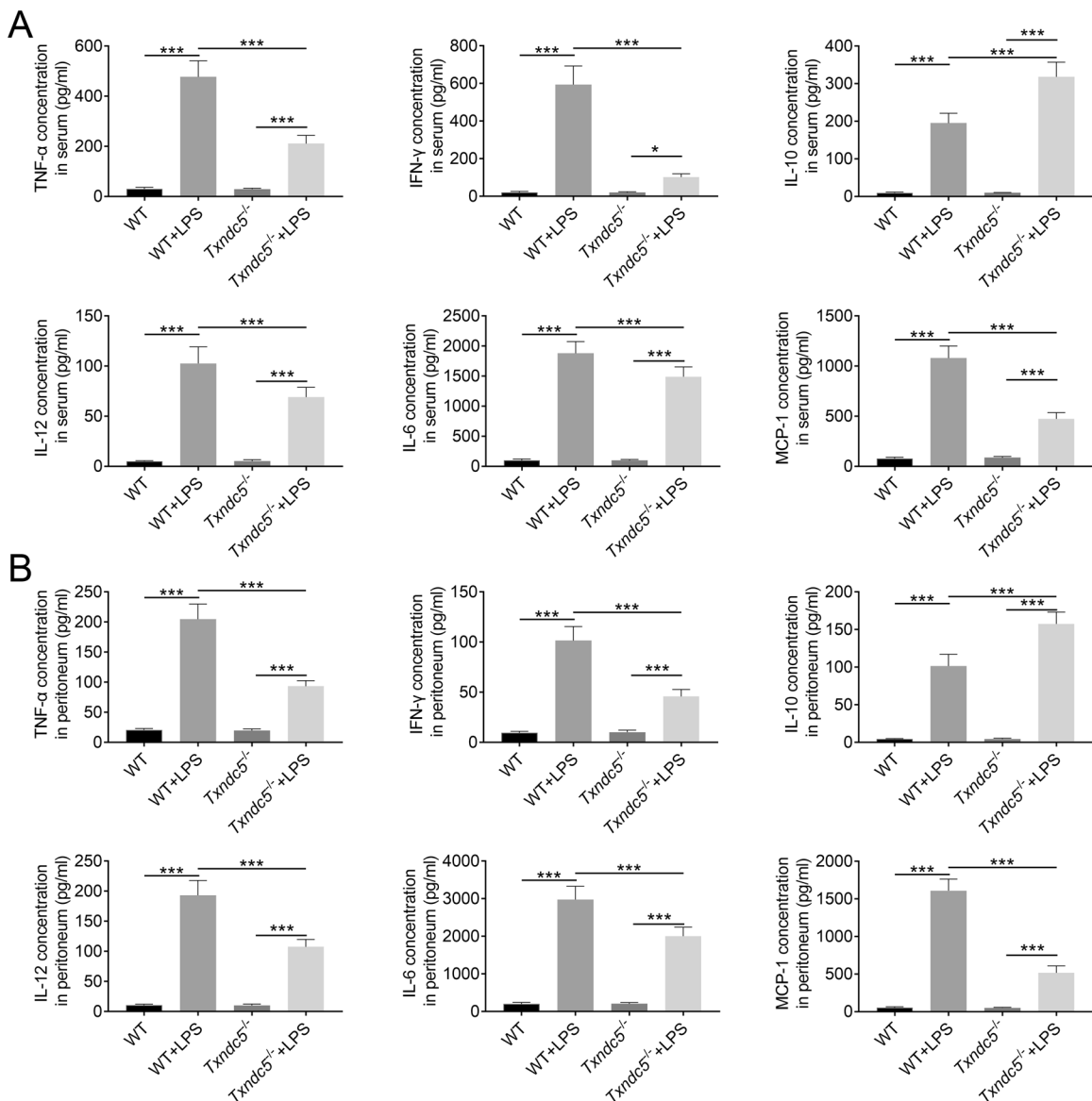


**Fig. 4** Effect of *Txn5* depletion on sepsis-induced inflammatory cytokines production in vivo. **A**, **B** WT and *Txn5*<sup>-/-</sup> mice were intraperitoneally injected with LPS (10 mg/kg body weight) or an equal volume of PBS. The blood samples and peritoneal tissues were collected from each animal immediately after death or euthanasia. The protein levels of TNF- $\alpha$ , IFN- $\gamma$ , IL-10, IL-12, IL-6, and MCP-1 in the **A** blood and **B** peritoneal tissues were determined by ELISA ( $n = 8$  per group). \*\*\* $p < 0.001$ .

## Western blot

The harvested tissues and cultured cells were lysed in RIPA buffer containing phosphatase inhibitors and protease inhibitors (Pierce, Rockford, USA). Protein concentration was determined by BCA protein assay (Thermo Fisher Scientific). An equal volume of protein samples (20–50  $\mu$ g) was loaded to 12% SDS-PAGE and then transferred to polyvinylidene fluoride membranes (MilliporeSigma, Burlington, USA). After blocking with 5% non-fat milk for 1 h, membranes were incubated with the following antibodies overnight at 4 °C: TXNDC5 (1/1000, Sigma-Aldrich), I $\kappa$ B $\beta$  (1/1000, Abcam), p-I $\kappa$ B $\beta$  (1/1000, Abcam), p-p65 (1/1000, Cell Signaling, Boston, USA), p65 (1/1000, Cell Signaling), and GAPDH (1/2000, Abcam). The next day, membranes were incubated with horseradish peroxidase-conjugated secondary antibody for 2 h and then visualized using the ChemiDoc MP system (BioRad Laboratories, Hercules, USA). Protein band intensity was analyzed by ImageJ (NIH).

## Statistical analysis

Data were expressed as mean  $\pm$  standard deviation from three independent experiments, each performed in triplicate. The R software (version 3.5.3) and SPSS software (version 24.0) were used for statistical analysis. Student's *t*-test or one-way analysis of variance was used to compare the results among different groups.  $p < 0.05$  was considered statistically significant.

## RESULTS

### Serum TXNDC5 levels are upregulated in patients with septic shock

The whole-blood RNA expression profiles of septic shock and non-septic shock patients were downloaded from the GEO database

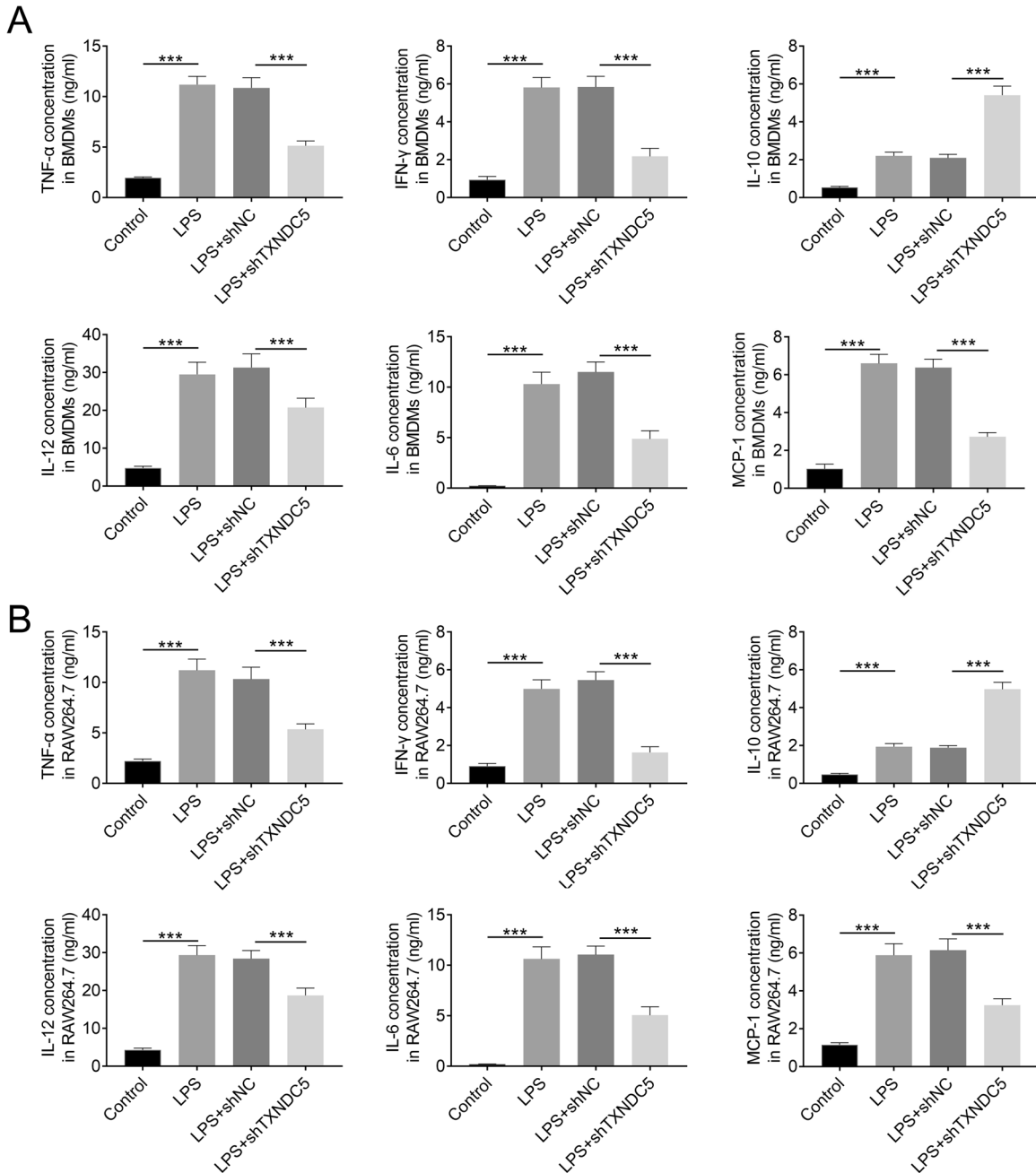


**Fig. 5** Effect of *TxnDC5* depletion on inflammatory responses in LPS-treated macrophages. **A, B** Mouse BMDMs and RAW264.7 cells were transfected with shRNA targeting TXNDC5 (shTXNDC5) of scrambled control sequence (shNC). WT and transfected macrophages were treated with 100 ng/mL of LPS for 12 h. The levels of TNF- $\alpha$ , IFN- $\gamma$ , IL-10, IL-12, IL-6, and MCP-1 in **A** BMDMs and **B** RAW264.7 cells were assessed by ELISA. \*\*\* $p < 0.001$ .

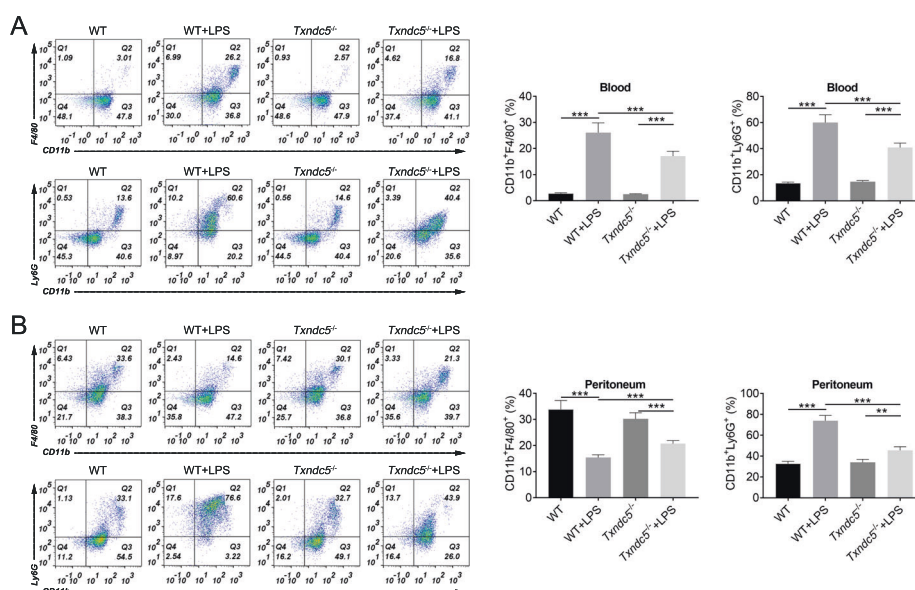


**Fig. 6** Effect of *Txnrc5* depletion on recruitment of immune cells into the blood and peritoneum. **A, B** WT and *Txnrc5*<sup>-/-</sup> mice were intraperitoneally injected with LPS (10 mg/kg body weight) or an equal volume of PBS. The blood samples and peritoneal fluids were collected from each animal immediately after death or euthanasia. Flow cytometry was performed to assess the percentages of macrophages (CD11b<sup>+</sup>F4/80<sup>+</sup>) and neutrophils (CD11b<sup>+</sup>Ly6G<sup>+</sup>) in the **A** blood and **B** peritoneal fluids ( $n = 8$  per group). \*\* $p < 0.01$ , \*\*\* $p < 0.001$ .

(GEO131761). The DEGs in septic shock are presented in a volcano plot (Fig. 1A). The heatmap analysis showed that TXNDC5 was one of the DEGs in septic shock (Fig. 1B). The expression of TXNDC5 in the samples from septic shock patients was significantly upregulated compared to the non-septic shock group (Fig. 1C). We further recruited 30 patients with sepsis (15 with septic shock, 15 without septic shock) and 15 healthy controls, and analyzed the expression of TXNDC5 in their PBMCs. The demographic and clinical characteristics of 30 septic patients are summarized in Table 1. Compared to healthy controls, both the non-septic shock and septic shock groups exhibited highly upregulated protein expression of TXNDC5, with more abundant expression observed in patients with septic shock (Fig. 1D). These data suggest that high TXNDC5 expression may be related to the severity of septic patients.

### TXNDC5 is upregulated in LPS-induced sepsis

To confirm the upregulation of TXNDC5 during the pathogenesis of sepsis, we established a mouse model of LPS-induced sepsis and investigated the expression of TXNDC5 at 12 h following LPS stimulation. TXNDC5 was highly expressed in the blood compared to other organs of mice (Fig. 2A). Then we measured the serum level of TXNDC5 in LPS-treated mice at different time points. The mRNA expression of TXNDC5 was significantly upregulated since 1 h after LPS stimulation and the highest level was observed at 6-h post injection (Fig. 2B). By comparing the protein expression of TXNDC5 in different organs of LPS-treated mice, we found that TXNDC5 was greatly upregulated in the liver, kidney, lung, and heart compared to other organs (Fig. 2C). Next, we treated BMDMs isolated from WT mice and RAW264.7 cells with or without LPS at different concentrations for 12 h. Compared to the control group, the expression of TXNDC5 was markedly increased in cells exposed to all concentrations of LPS, and the highest level was observed in the “100 ng/mL group” (Fig. 2D). Furthermore, the protein expression of TXNDC5 was significantly and time-dependently elevated in LPS-treated macrophages from 3 to 12 h post treatment, but downregulated at 24 h following stimulation (Fig. 2E). These findings demonstrate the upregulation of TXNDC5 in mice with LPS-induced sepsis and macrophages subjected to LPS stimulation.

### Target depletion of *Txnrc5* in vivo protects against sepsis-induced organ damage

To explore the effect of TXNDC5 expression on sepsis-related outcomes, we compared the survival and organ damage of WT and *Txnrc5*<sup>-/-</sup> mice following LPS injection. The survival curves showed that targeted depletion of *Txnrc5* improved the survival of mice with LPS-induced sepsis (Fig. 3A). Further histological examination of the lung, liver, kidney, and heart tissues revealed that LPS induced congestion, inflammatory cell infiltration, necrosis, and degeneration in these organs. *Txnrc5* knockout, however, alleviated LPS-induced histopathological organ damage in mice (Fig. 3B). Consistently, TUNEL staining (Fig. 3C) showed that LPS induced apoptosis in the lung (Fig. 3D), liver (Fig. 3E), kidney (Fig. 3F), and heart (Fig. 3G) tissues, while *Txnrc5* knockout alleviated LPS-induced apoptosis in mice. Therefore, we speculate that the inhibition of *Txnrc5* may exert a protective effect on the development of sepsis.

### *Txnrc5* depletion reduces sepsis-induced inflammatory cytokine production in mice

To examine the effect of *Txnrc5* depletion on sepsis-induced inflammatory responses, we compared the expression levels of inflammatory cytokines in the blood and peritoneal tissues of WT and *Txnrc5*<sup>-/-</sup> mice following LPS stimulation. Compared to PBS-treated group, all tested cytokines, including TNF- $\alpha$ , IFN- $\gamma$ , IL-10, IL-12, IL-6, and MCP-1, were highly upregulated in the blood and peritoneal tissues of WT mice following LPS injection. Treatment with LPS also significantly induced the production of all cytokines in the blood and peritoneal tissues of *Txnrc5*<sup>-/-</sup> mice, but to an extent that was significantly lower than the WT strain, except for IL-10, the anti-inflammatory cytokine (Fig. 4A, B).

### *Txnrc5* knockdown suppresses inflammatory responses in LPS-treated macrophages

To ascertain the beneficial role of TXNDC5 inhibition in sepsis-induced inflammation, we further examined the effect of *Txnrc5* knockdown on LPS-induced inflammatory cytokine production in vitro. LPS treatment significantly upregulated the production of TNF- $\alpha$ , IFN- $\gamma$ , IL-10, IL-12, IL-6, and MCP-1 in BMDMs and RAW264.7 cells. The knockdown of *Txnrc5*, however, effectively suppressed

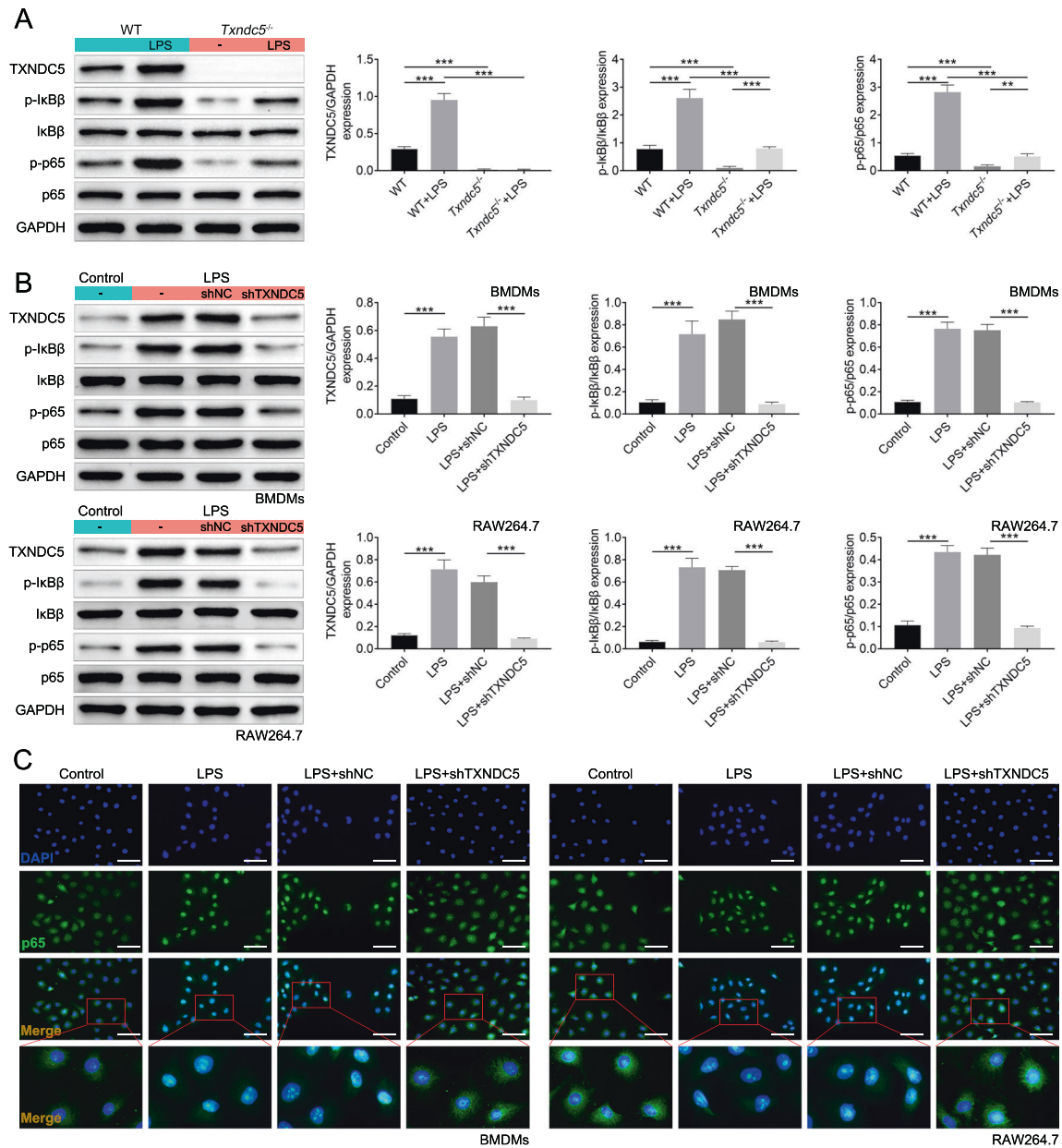


**Fig. 7** Effect of *Txndc5* depletion on the activity of NF- $\kappa$ B signaling in LPS-induced sepsis. **A** WT and *Txndc5*<sup>-/-</sup> mice were administered with LPS (10 mg/kg body weight) or an equal volume of PBS via intraperitoneal injection. The protein expressions of TXND5, p-I $\kappa$ B $\beta$ , I $\kappa$ B $\beta$ , p-p65, and p65 in the peritoneal tissues were assessed by western blot ( $n = 8$  per group). **B**, **C** BMDMs and RAW264.7 cells were transfected with shRNA against TXND5 shTXND5 or scrambled control sequence (shNC). WT and transfected macrophages were treated with 100 ng/mL of LPS for 12 h. **B** The protein expressions of TXND5, p-I $\kappa$ B $\beta$ , I $\kappa$ B $\beta$ , p-p65, and p65 were measured by western blot. **C** Immunofluorescence staining was performed to detect the expression of p65 in the cytoplasm and nuclei (DAPI: blue; p65: green). \*\* $p < 0.01$ , \*\*\* $p < 0.001$ .

LPS-induced upregulation of proinflammatory cytokines (i.e., TNF- $\alpha$ , IFN- $\gamma$ , IL-12, IL-6, and MCP-1) and promoted the production of anti-inflammatory cytokine IL-10 (Fig. 5A, B). Taken together, the above results imply that inhibition of TXND5 reduces LPS-triggered inflammatory responses in mice and cultured macrophages.

#### ***Txndc5* depletion affected the recruitment of macrophages and neutrophils into the blood and peritoneum**

To investigate the effect of *Txndc5* depletion in sepsis-induced immune cell recruitment, we analyzed the recruitment of macrophages (CD11b<sup>+</sup>F4/80<sup>+</sup>) and neutrophils (CD11b<sup>+</sup>Ly6G<sup>+</sup>) in the blood and peritoneal fluids of WT and *Txndc5*<sup>-/-</sup> mice following LPS injection. A significant increase in the percentages

of both macrophages and neutrophils was observed in WT septic mice compared to PBS-treated controls, indicating that LPS activated immune responses in vivo. The depletion of *Txndc5* partially but significantly reduced immune cell recruitment in LPS-treated mice (Fig. 6A). Moreover, LPS stimulation induced the recruitment of neutrophils, but not macrophages, into the peritoneum of WT mice. The knockout of *Txndc5*, however, significantly promoted migration of macrophages but decreased recruitment of neutrophils into the peritoneum compared to WT mice subjected to LPS treatment (Fig. 6B). These data show that *Txndc5* depletion not only reduced sepsis-induced macrophage recruitment and neutrophil infiltration into the blood, but also promoted the recruitment of macrophages into the peritoneum in response to LPS-induced sepsis.



### ***Txndc5* depletion alleviates LPS-induced sepsis by inhibiting the NF- $\kappa$ B signaling pathway**

Finally, we explored whether *Txndc5* depletion would affect the activity of NF- $\kappa$ B signaling in sepsis. Western blot analysis showed that LPS upregulated TXNDC5 and induced the activation of the NF- $\kappa$ B pathway in the peritoneal tissues of WT mice. The knockout of *Txndc5*, however, completely inhibited the phosphorylation of I $\kappa$ B $\beta$  and p65 following LPS injection (Fig. 7A). LPS treatment also activated the NF- $\kappa$ B signaling in cultured BMDMs and RAW264.7 cells. However, *Txndc5* deficiency suppressed the phosphorylation of I $\kappa$ B $\beta$  and p65 to a level similar to that observed in the untreated control groups (Fig. 7B). Furthermore, immunofluorescence staining showed that *Txndc5* knockdown in macrophages inhibited nuclear translocation of p65 in response to LPS stimulation (Fig. 7C). Collectively, *Txndc5* depletion inhibits sepsis-induced activation of the NF- $\kappa$ B signaling pathway.

## **DISCUSSION**

Sepsis and septic shock are pathological conditions developed from excessive host immune activation<sup>25</sup>. However, strategies that modulate aberrant host responses have been unsuccessful in a vast number of clinical trials, partially due to inadequate selection of therapeutic targets<sup>26</sup>. In this study, we proposed the potential of TXNDC5 as a promising therapeutic target for sepsis. Our data showed that the inhibition of TXNDC5 attenuated inflammatory cell activation and repressed organ injury during sepsis via the NF- $\kappa$ B signaling.

TXNDC5 possesses both disulfide isomerase and chaperone activities, therefore, plays an essential role in cell physiology and pathology<sup>27</sup>. The upregulation of TXNDC5 has been found in the blood and synovial tissues of RA patients and endothelial cells under hypoxic conditions to promote cell proliferation and angiogenesis<sup>28</sup>. Previous studies have also identified TXNDC5 as a tumor enhancer in multiple human malignancies, such as breast, liver, lung, colon, esophageal, and cervical cancers<sup>29</sup>. Here, the analysis of GEO data and blood samples from septic patients revealed that the expression of TXNDC5 in patients with septic shock was significantly higher than that of non-septic shock patients. Moreover, the *in vivo* sepsis model induced by LPS and cultured macrophages subjected to LPS stimulation showed significantly upregulated TXNDC5 expression compared with the corresponding controls, implying that TXNDC5 may play a role in the pathogenesis and severity of sepsis.

During sepsis, excessive immune responses often induce global hypoperfusion, tissue hypoxia, and, ultimately, organ dysfunction<sup>30</sup>. Multiple organ failure is a hallmark of sepsis associated with poor prognosis and increased in-hospital mortality<sup>31</sup>. The organs that are most frequently affected are the kidney, lung, liver, heart, and central nervous system<sup>32</sup>. Here, we first showed that TXNDC5 was dominantly expressed in the kidney, lung, liver, and heart of LPS-challenged mice. Moreover, by comparing the survival and organ injury of WT and *Txndc5*<sup>-/-</sup> mice following LPS injection, we found that *Txndc5* depletion improved the survival of LPS-treated mice and protected them against sepsis-induced organ damage.

Inflammatory cytokines are pleiotropic regulators of immune responses, involving in the pathophysiology of sepsis<sup>33</sup>. An exacerbated release of proinflammatory cytokines often results in dysregulated immune responses and subsequent tissue damage<sup>34</sup>. Therefore, a tightly regulated balance between proinflammatory and anti-inflammatory responses is crucial for eliminating invading pathogens and restricting excessive, tissue-damaging inflammation<sup>35</sup>. In this study, we reported that TXNDC5 deficiency repressed sepsis-induced upregulation of proinflammatory factors but promoted the expression of anti-inflammatory cytokine IL-10 in both mice and cultured macrophages treated with LPS, indicating that *Txndc5* depletion reduced sepsis-induced hyper-inflammatory responses.

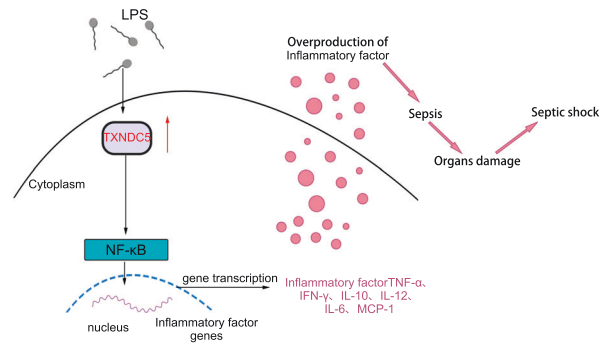


**Fig. 8** The mechanism diagram of TXNDC5 knockout suppressing septic shock. TXNDC5 inhibition attenuates LPS-induced septic shock in mice by inhibiting the NF- $\kappa$ B signaling pathway.

Macrophages and neutrophils are prominent pathogen scavengers in inflammation responses to infection and tissue injuries<sup>36</sup>. They are the predominant source of inflammatory cytokines and constitute major cell populations in the peritoneum of septic mice<sup>22</sup>. In our study, *Txndc5* knockout diminished macrophage and neutrophil activation in the systemic blood circulation, and enhanced recruitment of macrophages into the peritoneum of septic mice, which probably contributed to the enhanced pathogen clearance ability in *Txndc5*<sup>-/-</sup> mice relative to the WT controls.

The suppression of NF- $\kappa$ B activation is a potent strategy for regulating immune responses involved in sepsis-induced multiple organ failure<sup>37</sup>. TXNDC5 has been reported to modulate the activity of inflammatory signaling pathways in different diseases. A study of pulmonary fibrosis reported that TXNDC5 augmented transforming growth factor beta 1 signaling activity in lung fibroblasts, thereby promoting fibroblast proliferation and extracellular matrix production<sup>38</sup>. Also, TXNDC5 synergizes with heat shock cognate 70 protein, activating the NF- $\kappa$ B signaling by destabilizing the I $\kappa$ B $\beta$  protein in RA synovial fibroblasts<sup>16</sup>. Our data suggested that *Txndc5* knockout inhibited LPS-induced activation of the NF- $\kappa$ B signaling possibly by inhibiting the phosphorylation of I $\kappa$ B $\beta$  and p65, and subsequent nuclear translocation of p65 (Fig. 8). Further studies are needed to explore whether TXNDC5 would affect other NF- $\kappa$ B-related signaling pathways. Also, the beneficial effect of *Txndc5* depletion on inflammatory cells could be validated by transplanting *Txndc5*<sup>-/-</sup> bone marrow cells into WT hosts.

In conclusion, targeted depletion of TXNDC5 ameliorated LPS-induced sepsis by regulating the secretion of inflammatory cytokines and the recruitment of immune cells. The suppression of NF- $\kappa$ B activity by TXNDC5 deficiency may contribute to a better outcome of sepsis. These findings suggest that the inhibition of TXNDC5 may be a potential therapeutic strategy for the treatment of sepsis and related syndromes.

## **REFERENCES**

- Sagy, M., Al-Qaqa, Y. & Kim, P. Definitions and pathophysiology of sepsis. *Curr. Probl. Pediatr. Adolesc. Health Care* **43**, 260–263 (2013).
- Aragón-Benedí, C. et al. Methylene blue? Therapeutic alternative in the management of septic shock refractory to norepinephrine. *Signa. Vitae* **16**, 199–202 (2020).
- Delano, M. J. & Ward, P. A. The immune system's role in sepsis progression, resolution, and long-term outcome. *Immunol. Rev.* **274**, 330–353 (2016).
- Gaieski, D. F. & Goyal, M. What is sepsis? What is severe sepsis? What is septic shock? Searching for objective definitions among the winds of doctrines and wild theories. *Expert. Rev. Anti. Infect. Ther.* **11**, 867–871 (2013).
- De Backer, D., Orbegozo Cortes, D., Donadello, K. & Vincent, J. L. Pathophysiology of microcirculatory dysfunction and the pathogenesis of septic shock. *Virulence* **5**, 73–79 (2014).

6. Mayr, F. B., Yende, S. & Angus, D. C. Epidemiology of severe sepsis. *Virulence* **5**, 4–11 (2014).
7. Cheng, Y., Marion, T. N., Cao, X., Wang, W. & Cao, Y. Park 7: a novel therapeutic target for macrophages in sepsis-induced immunosuppression. *Front. Immunol.* **9**, 2632 (2018).
8. Dickson, K. & Lehmann, C. Inflammatory response to different toxins in experimental sepsis models. *Int. J. Mol. Sci.* **20**, 4341 (2019).
9. Kany, S., Vollrath, J. T., & Relja B. Cytokines in inflammatory disease. *Int. J. Mol. Sci.* **20**, 6008 (2019).
10. Chousterman, B. G., Swirski, F. K. & Weber, G. F. Cytokine storm and sepsis disease pathogenesis. *Semin. Immunopathol.* **39**, 517–528 (2017).
11. Orecchioni, M., Ghosheh, Y., Pramod, A. B. & Ley, K. Macrophage polarization: different gene signatures in M1(LPS+) vs. classically and m2(LPS-) vs. alternatively activated macrophages. *Front. Immunol.* **10**, 1084 (2019).
12. Fujino, G., Noguchi, T., Takeda, K. & Ichijo, H. Thioredoxin and protein kinases in redox signaling. *Semin. Cancer Biol.* **16**, 427–435 (2006).
13. Shih, Y. C. et al. Endoplasmic reticulum protein TXNDC5 augments myocardial fibrosis by facilitating extracellular matrix protein folding and redox-sensitive cardiac fibroblast activation. *Circ. Res.* **122**, 1052–1068 (2018).
14. Horna-Terrón, E., Pradilla-Dieste, A., Sánchez-de-Diego, C. & Osada, J. TXNDC5, a newly discovered disulfide isomerase with a key role in cell physiology and pathology. *Int. J. Mol. Sci.* **15**, 23501–23518 (2014).
15. Chawsheen, H. A., Ying, Q., Jiang, H. & Wei, Q. A critical role of the thioredoxin domain containing protein 5 (TXNDC5) in redox homeostasis and cancer development. *Genes Dis.* **5**, 312–322 (2018).
16. Wang, L. et al. TXNDC5 synergizes with HSC70 to exacerbate the inflammatory phenotype of synovial fibroblasts in rheumatoid arthritis through NF- $\kappa$ B signaling. *Cell. Mol. Immunol.* **15**, 685–696 (2018).
17. World Medical Association. World Medical Association Declaration of Helsinki: ethical principles for medical research involving human subjects. *JAMA* **310**, 2191–2194 (2013).
18. National Research Council Committee for the Update of the Guide for the Care and Use of Laboratory Animals. *The National Academies Collection: Reports Funded by National Institutes of Health. Guide for the Care and Use of Laboratory Animals.* (National Academies Press (US), National Academy of Sciences; Washington (DC), 2011).
19. Xu, C. et al. Identification of key genes and novel immune infiltration-associated biomarkers of sepsis. *Innate. Immun.* **26**, 666–682 (2020).
20. Singer, M. et al. The third international consensus definitions for sepsis and septic shock (Sepsis-3). *JAMA* **315**, 801–810 (2016).
21. Swamydas, M., Luo, Y., Dorf, M. E. & Lionakis, M. S. Isolation of mouse neutrophils. *Curr. Protoc. Immunol.* **110**, 3.20.21–23.20.15 (2015).
22. Bai, J. et al. TAT-SNAP-23 treatment inhibits the priming of neutrophil functions contributing to shock and/or sepsis-induced extra-pulmonary acute lung injury. *Innate. Immun.* **21**, 42–54 (2015).
23. Zhang, Q. et al. Novel pharmacological inhibition of EZH2 attenuates septic shock by altering innate inflammatory responses to sepsis. *Int. Immunopharmacol.* **76**, 105899 (2019).
24. Wang, J., et al. iNOS interacts with autophagy receptor p62 and is degraded by autophagy in macrophages. *Cells* **8**, 1255 (2019).
25. Rhodes, A. et al. Surviving Sepsis Campaign: international guidelines for management of sepsis and septic shock: 2016. *Intensive Care Med.* **43**, 304–377 (2017).
26. van der Poll, T., van de Veerdonk, F. L., Scicluna, B. P. & Netea, M. G. The immunopathology of sepsis and potential therapeutic targets. *Nat. Rev. Immunol.* **17**, 407–420 (2017).
27. Galligan, J. J. & Petersen, D. R. The human protein disulfide isomerase gene family. *Hum. Genomics* **6**, 6 (2012).
28. Chang, X. et al. Investigating a pathogenic role for TXNDC5 in rheumatoid arthritis. *Arthritis Res. Ther.* **13**, R124 (2011).
29. Chang, X. et al. Investigating a pathogenic role for TXNDC5 in tumors. *Int. J. Oncol.* **43**, 1871–1884 (2013).
30. Pool, R., Gomez, H. & Kellum, J. A. Mechanisms of organ dysfunction in sepsis. *Crit. Care Clin.* **34**, 63–80 (2018).
31. Caraballo, C. & Jaimes, F. Organ dysfunction in sepsis: an ominous trajectory from infection to death. *Yale J. Biol. Med.* **92**, 629–640 (2019).
32. Rossaint, J. & Zarbock, A. Pathogenesis of multiple organ failure in sepsis. *Crit. Rev. Immunol.* **35**, 277–291 (2015).
33. Chaudhry, H. et al. Role of cytokines as a double-edged sword in sepsis. *In Vivo* **27**, 669–684 (2013).
34. Cao, C., Yu, M. & Chai, Y. Pathological alteration and therapeutic implications of sepsis-induced immune cell apoptosis. *Cell Death Dis.* **10**, 782 (2019).
35. Schulte, W., Bernhagen, J. & Bucala, R. Cytokines in sepsis: potent immunoregulators and potential therapeutic targets—an updated view. *Mediators Inflamm.* **2013**, 165974 (2013).
36. Su, Y., Gao, J., Kaur, P., & Wang, Z. Neutrophils and macrophages as targets for development of nanotherapeutics in inflammatory diseases. *Pharmaceutics* **12**, 1222 (2020).
37. Park, S. D. et al. Intranuclear interactomic inhibition of NF- $\kappa$ B suppresses LPS-induced severe sepsis. *Biochem. Biophys. Res. Commun.* **464**, 711–717 (2015).
38. Lee, T. H. et al. Fibroblast-enriched endoplasmic reticulum protein TXNDC5 promotes pulmonary fibrosis by augmenting TGF $\beta$  signaling through TGFBR1 stabilization. *Nat. Commun.* **11**, 4254 (2020).

#### AUTHOR CONTRIBUTIONS

Y. Z. and W. M. designed the study and supervised the data collection. C. M. analyzed and interpreted the data. X. R. and Y. W. prepared the manuscript for publication and reviewed the draft of the manuscript. All authors have read and approved the manuscript.

#### COMPETING INTERESTS

The authors declare no competing interests.

#### ETHICS APPROVAL

All procedures performed in studies involving human participants were in accordance with the standards upheld by the Ethics Committee of the Shaoxing Central Hospital Medical Alliance General Hospital and with those of the 1964 Helsinki Declaration and its later amendments for ethical research involving human subjects. All animal experiments were approved by the Ethics Committee of the Shaoxing Central Hospital Medical Alliance General Hospital for the use of animals and conducted in accordance with the National Institutes of Health Laboratory Animal Care and Use Guidelines.

#### INFORMED CONSENT

Written informed consent was obtained from a legally authorized representative(s) for anonymized patient information to be published in this article.

#### ADDITIONAL INFORMATION

**Correspondence** and requests for materials should be addressed to Yanping Zeng.

**Reprints and permission information** is available at <http://www.nature.com/reprints>

**Publisher's note** Springer Nature remains neutral with regard to jurisdictional claims in published maps and institutional affiliations.